EasyChair Preprint

№ 4721

Comparison of Two Convolutional Neural Network Models for Automated Classification of Brain Cancer Types

Muhammad Shofi Fuad, Choirul Anam, Kusworo Adi and Geoff Dougherty

EasyChair preprints are intended for rapid dissemination of research results and are integrated with the rest of EasyChair.

December 9, 2020

Comparison of Two Convolutional Neural Network Models for Automated Classification of Brain Cancer Types

Muhammad Shofi Fuad[1*], Choirul Anam[1], Kusworo Adi, and Geoff Dougherty[2]

[1]*Department of Physics, Faculty of Sciences and Mathematics, Diponegoro University, Jl. Prof. Soedarto SH, Tembalang, Semarang 50275, Central Java, Indonesia.*
[2] *Department of Applied Physics and Medical Imaging, California State University Channel Islands, Camarillo, CA 93012, USA.*

* *Email: shofimuhammadfuad@gmail.com*

ABSTRACT

Background: Convolutional neutral network (CNN) is widely used in the classification of brain cancer types and many architectures of the CNN have been developed. Comparasions of various architectures on a specific clinical task is essential.

Objective: This study aims to compare a deep transfer learning model with AlexNet and GoogleNet architectures for brain tumor classification on the T1-w magnetic resonance imaging (MRI) images.

Material and Methods: The comparison of the AlexNet and the GoogleNet architectures was implemented on the T1-w MRI images with three tumor types: glioma, meningioma and pituitary. The total images were 3,064 consisted of 1,426 gliomas, 708 meningiomas, and 930 pituitaries. 80% of datasets were for training and 20% of datasets were for testing.

Results: It is found that the accuracies for the AlexNet is 94.6% and for the GoogleNet is 92%. The sensitivity, specificity, precision and recall for the AlexNet are 94%, 95.2%, 94.6% and 46.9%, respectively. While sensitivity, specificity, precision and recall for the GoogleNet are 96.3%, 96.8%, 87.3% and 45.9%, respectively.

Conclusion: Comparison of the AlexNet and the GoogleNet architectures to classify tree types of brain tumors from T1-w MRI images has been performed. It is found that the both architectures produce accuracies more than 90%. However, the AlexNet architecture is superior compared to the GoogleNet architecture.

Keywords*:* Convolutional neural network, transfer learning, AlexNet, GoogleNet, brain tumor classification

1. Introduction

A convolutional neural network (CNN) is one of the image processing techniques widely used in medical image analysis. The CNN is inspired by the performance of the human brain that can distinguish various objects by visualizing them [1]. The CNN has a good performance in classifying images [2]. Previous studies showed that the accuracy of the CNN reached 99.9% for diagnosing breast cancer [3], 99.6% for classification of cataract [4], 98.7% for the classification of brain tumors (Deepak and Ameer, 2019), and 91.28% for classification of meningioma tumors, gliomas, and pituitary tumors [6].

Many models have been developed for the CNN, such as AlexNet, GoogleNet, ResNet, InceptionV3, CapsNet, etc. Classification of 5 classes of degenerative, inflammatory, normal, cerebrovascular and neoplastic brain diseases had been performed using various models with different accuracies, i.e., 84.11% for AlexNet, 90.65% for ResNet18, 91.39% for ResNet34 and 96.26% for ResNet50 [7]. The InceptionV3 had been used and distinguished between benign and malignant kidney tumors on CT images [8]. The CapsNet or classification of three types of tumors gets an accuracy of 90.89% [9].

The performance of the CNN with a large dataset certainly need length of image processing time. Therefore, there is a need for an approach to accelerate the processing time. One approach is by implementation of the transfer learning (TL). The TL approach has been proven to achieve outstanding classification performance with an accuracy rate of 97.86% for brain disorders and 91.37% for breast cancer [10, 11, 3].

The classifications of brain cancer types using CNN applications are widely exlored [6, 9, 12]. The main purpose of brain cancer classification is to obtain clinical information about the presence, location, and type of tumor. The important information be used for the correct diagnosis and treatment [13]. Although many models had been performed, however their evaluations are sometime performed on each individual architecture separately from other architectures. Comparison various architectures of the CNN in clasisification of brain tumor types for the same datasets is essntial. Therefore, the purpose of this study is to compare the classification system of the AlexNet and the GoogleNet to classify types of meningioma brain tumors, meningiomas, and pituitary tumors from the magnetic resonance imaging (MRI).

2. Materials and Methods

2.1 Dataset

T1-w brain MRI datasets were obtained from Nanfang Hospital, Guangzhou, China, and General Hospital, Tianjing Medical University, China, from 2005 to 2010. The datasets were freely obtained from the link: https://github.com/chengjun583/brainTumorRetrieval. The total image data was 3064 slices from 233 patients, containing 708 meningiomas, 1426 gliomas, and 930 pituitary tumors. The images had a resolution of 512 × 512 pixels with a size of every pixel was 0.49 × 0.49 mm^2. The thickness of every slice was 6 mm and the slit gap was 1 mm [6].

The datasets were provided in the MATLAB data format. Each file stored variables that contain data information:

cjdata.label: 1 for meningioma, 2 for glioma, 3 for pituitary tumors

cjdata.PID: patient ID

cjdata.image: image data

cjdata.tumorBorder: vector that stores discrete point coordinates at the tumor boundary.

cjdata.tumorMask: binary image with 1s showing the tumor region

Each original image was resized from 512 × 512 to 224 × 224 with three different kernels, so that it became 224 × 224 × 3.

2.2 Deep transfer learning

Two architectures of the AlexNet and the GoogleNet will be examined and compared in this study. The transfer learning (TL) was used to improve the CNN model with two architectures. This TL technique was expected to speed up training time and improve accuracy. The TL method took fully connectivity (FC) as an image representation with two node Softmax layers and classification layers [7]. Other parameters of the original model were preserved and used as initializations. The entire structure was then divided into two parts: the pre-training network and the transferred network [14]. The scheme of the deep TL with AlexNet and GoogleNet architecture is shown in Figures 1 and 2. The difference between the AlexNet and the Googlenet was the layers used. The AlexNet had 25 layers while the GoogleNet had 22 layers. Another difference was indicated by the inception module on the GoogleNet while the AlexNet did not have it.

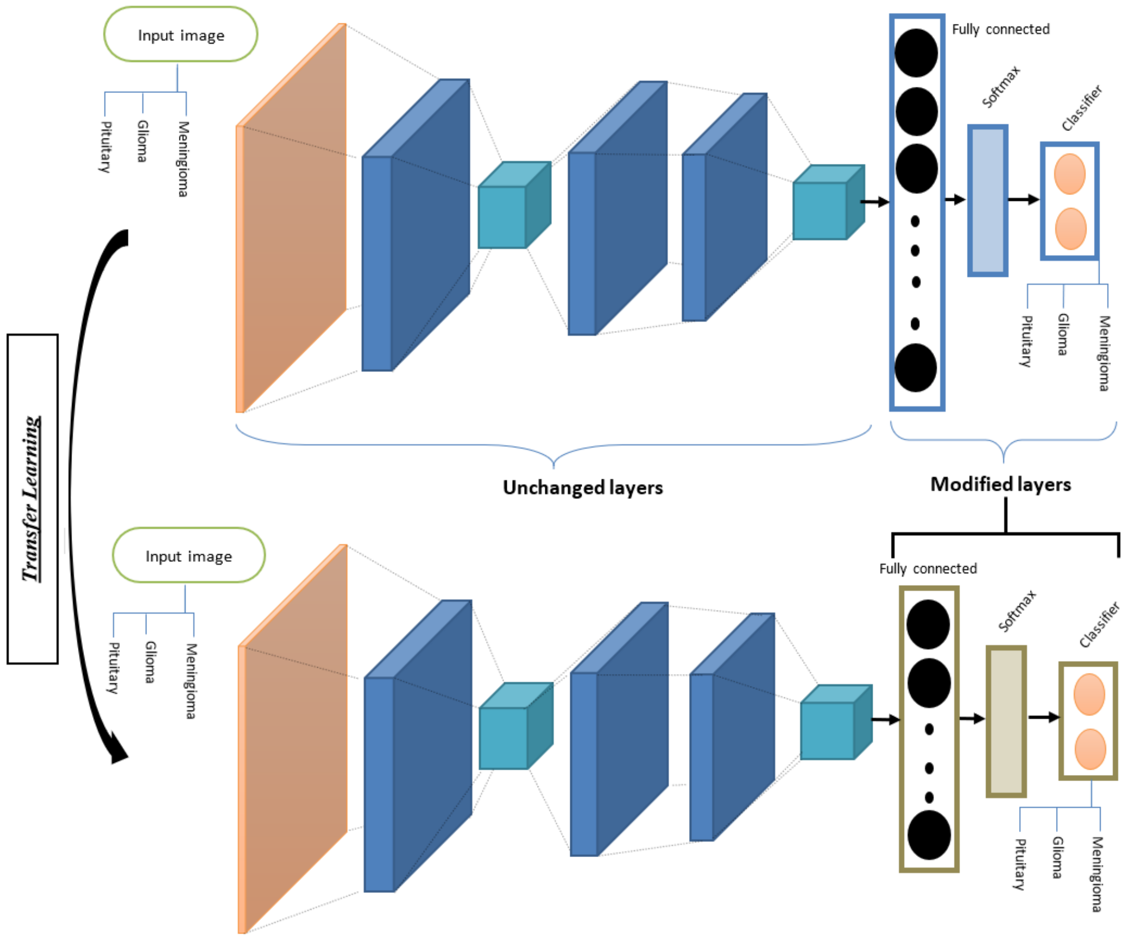

Parameters

Convolution Layer 1
- Filter size [11, 11]
- numFilter [96]
- Stride [4, 4]
- Dilatation Factor [1, 1]
- Padding [0, 0, 0, 0]

Convolution Layer 2
- Filter size [5, 5]
- numFilter [128]
- Stride [1, 1]
- Dilatation Factor [1, 1]
- Padding [2, 2, 2, 2]

Convolution Layer 3
- Filter size [3, 3]
- numFilter [192]
- Stride [1, 1]
- Dilatation Factor [1, 1]
- Padding [1, 1, 1, 1]

Convolution Layer 4
- Filter size [3, 3]
- numFilter [192]
- Stride [1, 1]
- Dilatation Factor [1, 1]
- Padding [1, 1, 1, 1]

Convolution Layer 5
- Filter size [3, 3]
- numFilter [192]
- Stride [1, 1]
- Dilatation Factor [1, 1]
- Padding [1, 1, 1, 1]

: Input Image

: Convolution layer

: Max Pooling
- Filter 3 x 3

Figure 1. AlexNet architecture.

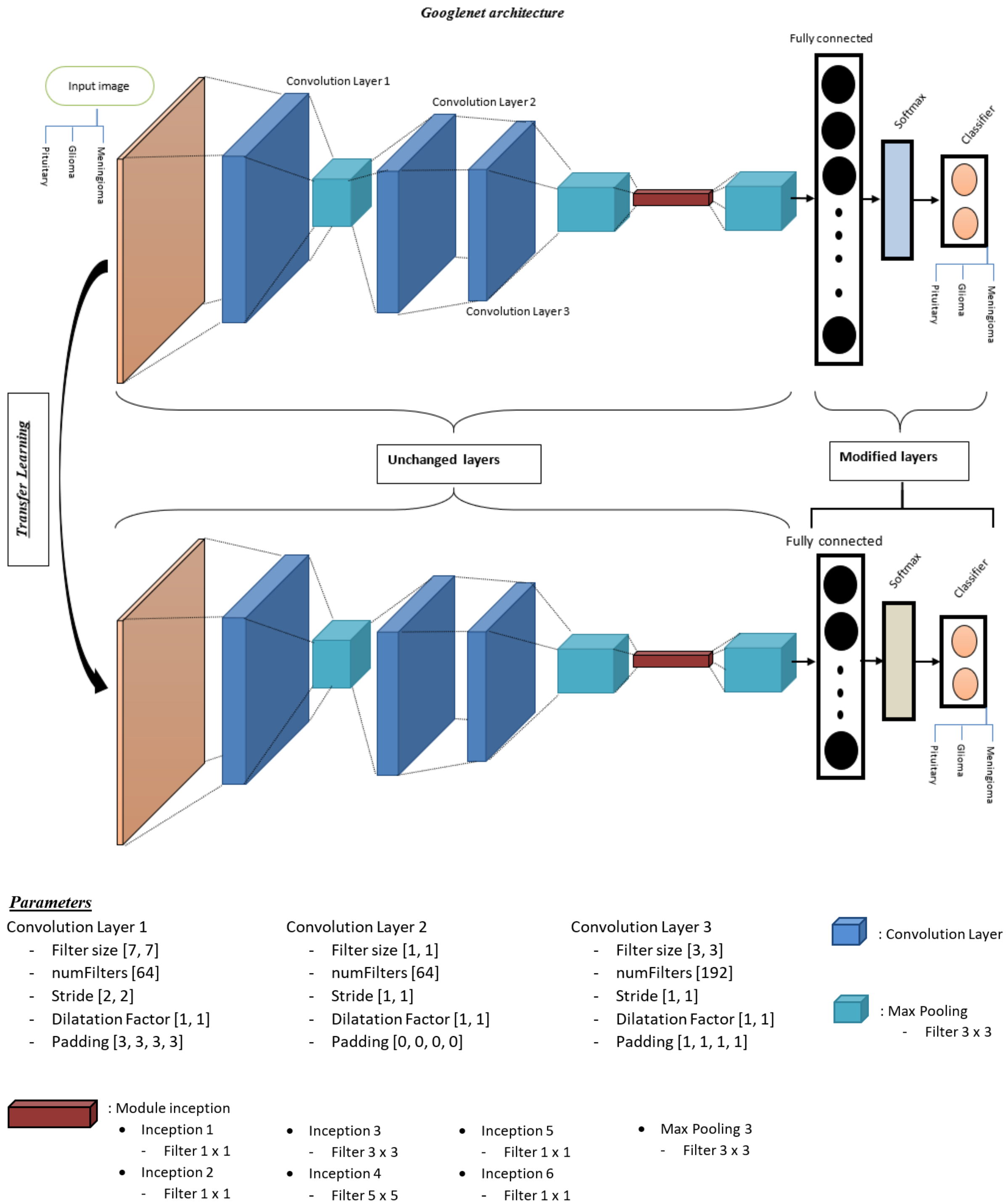

Figure 2. GoogleNet architecture.

2.3 Identification process

This study compared classification systems of brain tumor types on MRI images based on the AlexNet and the GoogleNet architectures with the TL approach. The stages in this study can be seen in Figure 3.

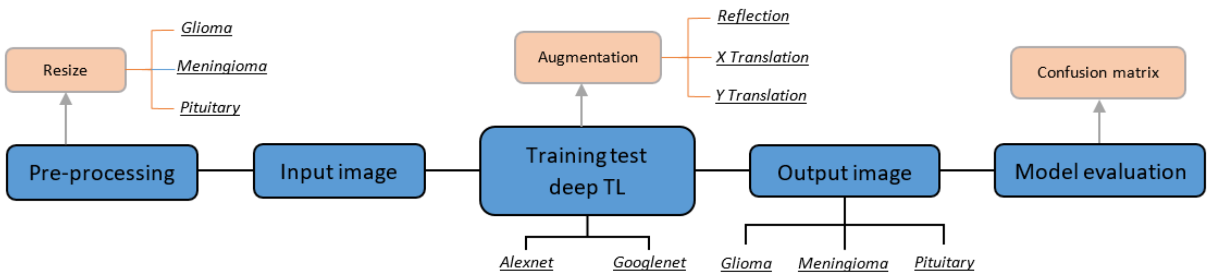

Figure 3. A block diagram representation of classification using the AlexNet and the GoogleNet architectures.

The training was conducted using a TL approach using stochastic gradient derivatives with batch size 128, momentum 0.9 and weight decay 0.0005. The training was conducted with a learning rate of 0.0001. Network training was carried out around 30 epochs. The image was processed in convolution with the AlexNet and the GoogleNet architectures to obtain accuracy values in image processing. In the training process, augmentation techniques were given in an effort to improve validation and better accuracy [15, 16]. A classification model used the Sofmax function to get more than one class of output. While the layer classification function was governed by default to define the output class of the trained image.

80% datasets were for training and 20% datasets were for testing. Classification performance evaluation was measured and displayed in *confusion matrix*. The representation of *confusion matrix* performance measurement was divided into six parts: accuracy, error rate, sensitivity, specificity, precision and recall. Parameters were tabulated in Table 1.

In this study, the Acer Swift-3 Laptop with Windows 10 Ori 64-bit operating system and with the Intel® core ™ i3-7020U RAM 20GB, 256GB SSD and Graphics Processing Unit NVIDIA ™ GeForce MX 150M type with 2.3 GHz computing capability were used. Comparison was implemented in MATLAB 2019b.

Table 1. Performance parameters, formula and evaluation focus of each parameter.

Performance parameter	**Formula**	**Evaluation focus**
Accuracy	$\frac{\sum_{i=1}^{l}\frac{TP_i+TN_i}{TP_i+FP_i+TN_i+FN_i}}{l}$	Measures the ratio of correct predictions to the total number of instances evaluated.
Error rate	$\frac{\sum_{i=1}^{l}\frac{FP_i+FN_i}{Tp_i+FP_i+TN_i+FN_i}}{l}$	Measures the ratio of incorrect predictions to the total number of instances evaluated.
Sensitivity	$\frac{\sum_{i=1}^{l}\frac{TP_i}{TP_i+FN_i}}{l}$	Measures the fraction of positive patterns that are correctly classified
Specificity	$\frac{\sum_{i=1}^{l}\frac{TN_i}{TN_i+FP_i}}{l}$	Measures the fraction of negative patterns that are correctly classified.
Precision	$\frac{\sum_{i=1}^{l}\frac{TP_i}{TP_i+FP_i}}{l}$	Measures the positive patterns that are correctly predicted from the total predicted patterns in a positive class.
Recall	$\frac{\sum_{i=1}^{l}\frac{TP_i}{TP_i+TN_i}}{l}$	Measures the fraction of positive patterns that are correctly classified

Where *TP* is true positive, *FP* is false negative, *TN* is true negative and *FN* is false negative.

3. Results

The training times to complete 30 epochs with an iteration of 214 per epoch are 21 hours 30 minutes 10 seconds for the AlexNet and 48 hours 58 minutes 57 seconds for the GoogleNet.

3.1 *Training process*

Figure 4 shows the performance of the classification model during training for the AlexNet architecture. Figure 4(a) shows the graph of validation accuracy during training. The blue line is the classification model training and the dashed black line is the validation of the classification model. Figure 4(b) shows a graph of validation errors during training. The orange line is the classification model error and the dashed black line is the validation of the classification model error. In the training process, the AlexNet model achieves 94.55% validation accuracy and 5.45% error validation.

Figure 5 shows the performance of the classification model during training for the GoogleNet architecture. Figure 5(a) shows the graph of validation accuracy during training, and Figure 5(b) shows a graph of validation errors during training. In the training process, the GoogleNet model achieves 91.99% validation accuracy and 8.01% error validation.

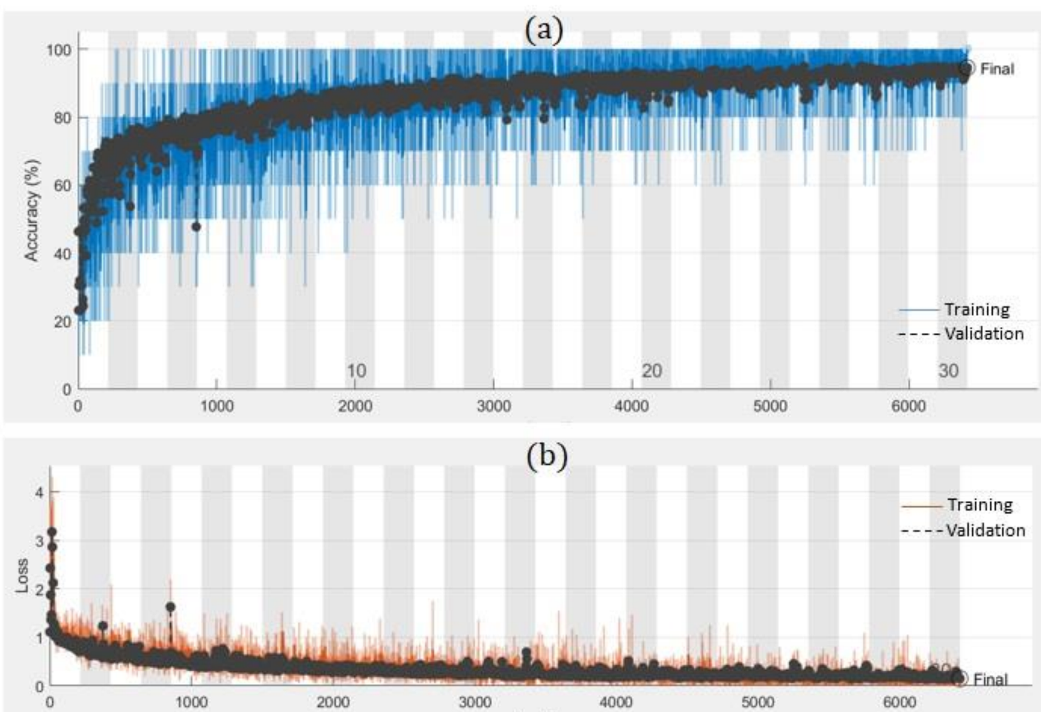

Figure 4. Classification results of the TL model with the AlexNet architecture. (a) validation accuracy and (b) loss validation.

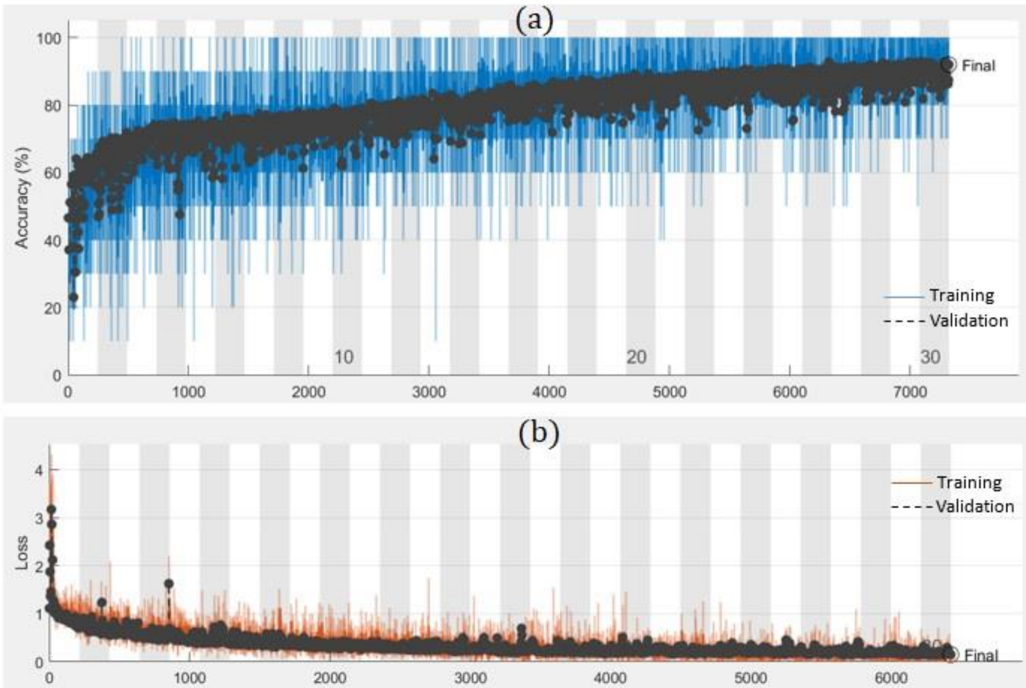

Figure 5. **C**lassification results of the TL model with the GoogleNet architecture. (a) validation accuracy and (b) loss validation.

3.2 Performance classification

The results of the *confusion matrix* are shown in Figure 6. The performance results of the *confusion matrix* classification show a summary of predictions made by the model, where each row represents the actual class and each column represents the prediction class. From the confusion matrices Figure 6, performance of measurement parameters in terms of *accuracy*, *error rate*, *sensitivity*, *specificity*, *precision*, and *recall* for the AlexNet and the GoogleNet architectures are tabulated in Table 2.

Table 1. The results of the performances for the AlexNet and GoogleNet architectures.

Model	Accuracy	Error rate	Sensitivity	Specificity	Precision	Recall
AlexNet	94.6%	5.4%	94%	95.2%	94.6%	46.9%
GoogleNet	92%	8%	96.3%	96.8%	87.3%	45.9%

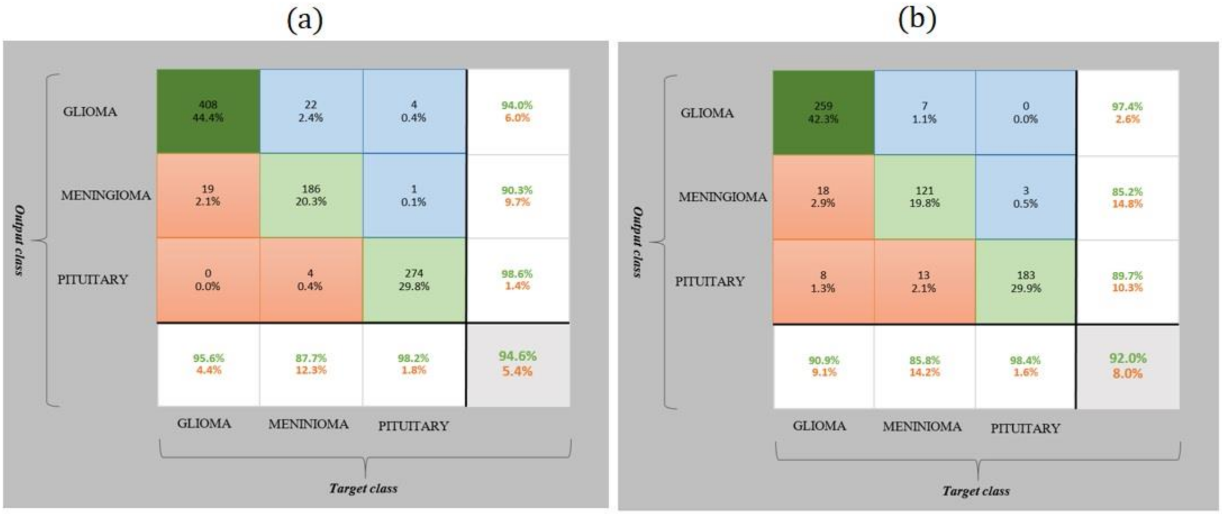

Figure 6. *Confusion matrix* classification model results. The first column of the first row indicates true positive. The second row of the second column and the third row of the third column indicates true negative. The first row of the second and third columns and the second row of the third column show false positivity. Row to the first two columns and rows to three of the first and second columns indicate false negatives. (a) Results of AlexNet architecture, and (b) Results of GoogleNet architecture.

4. Discussion

This study presents a comparison of the deep TL model of the AlexNet and GoogleNet architectures for the identification of three brain tumor types: gliomas, meningiomas and pituitary on T1-w MRI images from 3,064 MRI images. Augmentation techniques are applied to increase dataset size and increase accuracy. The augmentation technique applied is reflection and rotation on the X and Y axes.

The results showed that the Alexnet and the GoogleNet architectures result the accuracy rates of 94.6% and 92% for the Alexnet and GoogleNet architectures, respectively. In addition, training time for the AlexNet is faster than the GoogleNet. Therefore, AlexNet is considered superior in the brain tumor type classification compared to the GoogleNet.

Several studies [6, 9, 12] related to the model for automatically brain cancer types from T1-*w* MRI images are tabulated in Table 3. It shows that the AlexNet and GoogleNet are superior compared to Intensity Histogram, GLCM, BOW, Deep Learning CNN, and CapsNets. However, these comparisons are from different datasets. Comparisons for more models and architectures in the same datasets will be performed in a further study.

Table 2. Comparisons of classification studies for brain cancer.

Author	Year	Method	Accuracy
Cheng et al. [6]	2015	Intensity Histogram	87.5%
		GLCM	89.7%
		BOW	91.3%
Paul et al. [12]	2017	Deep Learning CNN	91.4%
Afshar et al. [9]	2018	CapstNets	90.9%
This study	2020	Alexnet	94.6%
		GoogleNet	92.0%

The AlexNet and GoogleNet achieved a higher accuracy than the previous models. This is because the transfer learning (TL) feature was added to the last three layers as replacement layers in the AlexNet and GoogleNet architectures. This is necessary because TL can improve the training process in one domain by transferring information from related domains by taking fully connectivity (FC) as an image representation with two Softmax layer nodes and a classification layer.

5. Conclusion

This research presents a comparison of the AlexNet and the GoogleNet architectures for automatic classification of brain cancer types from T1-w MRI images with deep TL models. Three types of brain tumors are glioma, meningioma and pituitary. According to the results of the performance of the classification system, this model has reached an accuracy value of 94.6% for AlexNet and 92% for GoogleNet.

6. Acknowledgments

This work was funded by the Riset Publikasi Internasional Bereputasi Tinggi (RPIBT), Diponegoro University. Contract Number: 329-116/UN7.P4.3/PP/2019).

References

[1] M. Vardhana, N. Arunkumar, S. Lasrado, E. Abdulhay, and G. Ramirez-Gonzalez, "Convolutional neural network for bio-medical image segmentation with hardware acceleration," *Cogn. Syst. Res.*, vol. 50, pp. 10–14, 2018, doi: 10.1016/j.cogsys.2018.03.005.

[2] M. M. Badža and M. C. Barjaktarović, "Classification of brain tumors from mri images using a convolutional neural network," *Appl. Sci.*, vol. 10, no. 6, 2020, doi: 10.3390/app10061999.

[3] S. Dabeer, M. M. Khan, and S. Islam, "Cancer diagnosis in histopathological image: CNN based approach," *Informatics Med. Unlocked*, vol. 16, no. May, p. 100231, 2019, doi: 10.1016/j.imu.2019.100231.

[4] B. K. Triwijoyo, W. Budiharto, and E. Abdurachman, "The Classification of Hypertensive Retinopathy using Convolutional Neural Network," *Procedia Comput. Sci.*, vol. 116, no. October, pp. 166–173, 2017, doi: 10.1016/j.procs.2017.10.066.

[5] S. Deepak and P. M. Ameer, "Brain tumor classification using deep CNN features via transfer learning," *Comput. Biol. Med.*, vol. 111, no. June, p. 103345, 2019, doi: 10.1016/j.compbiomed.2019.103345.

[6] J. Cheng *et al.*, "Enhanced performance of brain tumor classification via tumor region augmentation and partition," *PLoS One*, vol. 10, no. 10, pp. 1–13, 2015, doi: 10.1371/journal.pone.0140381.

[7] M. Talo, U. B. Baloglu, Ö. Yıldırım, and U. Rajendra Acharya, "Application of deep transfer learning for automated brain abnormality classification using MR images," *Cogn. Syst. Res.*, vol. 54, pp. 176–188, 2019, doi: 10.1016/j.cogsys.2018.12.007.

[8] S. Zhou, Y. Wang, T. Zhu, and L. Xia, "CT Features of Coronavirus Disease 2019 (COVID-19) Pneumonia in 62 Patients in Wuhan, China.," *AJR. Am. J. Roentgenol.*, no. October, pp. 1–8, 2020, doi: 10.2214/AJR.20.22975.

[9] P. Afshar, K. N. Plataniotis, and A. Mohammadi, "Capsule Networks for Brain Tumor Classification Based on MRI Images and Coarse Tumor Boundaries," *ICASSP, IEEE Int. Conf. Acoust. Speech Signal Process. - Proc.*, vol. 2019-May, pp. 1368–1372, 2019, doi: 10.1109/ICASSP.2019.8683759.

[10] M. Talo, O. Yildirim, U. B. Baloglu, G. Aydin, and U. R. Acharya, "Convolutional neural networks for multi-class brain disease detection using MRI images," *Comput. Med. Imaging Graph.*, vol. 78, p. 101673, 2019, doi: 10.1016/j.compmedimag.2019.101673.

[11] E. Deniz, A. Şengür, Z. Kadiroğlu, Y. Guo, V. Bajaj, and Ü. Budak, "Transfer learning based histopathologic image classification for breast cancer detection," *Heal. Inf. Sci. Syst.*, vol. 6, no. 1, 2018, doi: 10.1007/s13755-018-0057-x.

[12] J. S. Paul, A. J. Plassard, B. A. Landman, and D. Fabbri, "Deep learning for brain tumor classification," *Biomed. Appl. Mol. Struct. Funct. Imaging*, vol. 10137, no. 2, p. 1013710, 2017, doi: 10.1117/12.2254195.

[13] M. K. Abd-Ellah, A. I. Awad, A. A. M. Khalaf, and H. F. A. Hamed, "A review on brain tumor diagnosis from MRI images: Practical implications, key achievements, and lessons learned," *Magn. Reson. Imaging*, vol. 61, no. August 2018, pp. 300–318, 2019, doi: 10.1016/j.mri.2019.05.028.

[14] S. Lu, Z. Lu, and Y. D. Zhang, "Pathological brain detection based on AlexNet and

transfer learning," *J. Comput. Sci.*, vol. 30, pp. 41–47, 2019, doi: 10.1016/j.jocs.2018.11.008.

[15] A. Mikołajczyk and M. Grochowski, "2019 International Interdisciplinary PhD Workshop, IIPhDW 2019," *2019 Int. Interdiscip. PhD Work. IIPhDW 2019*, pp. 117–122, 2019.

[16] C. Shorten and T. M. Khoshgoftaar, "A survey on Image Data Augmentation for Deep Learning," *J. Big Data*, vol. 6, no. 1, 2019, doi: 10.1186/s40537-019-0197-0.

[17] P. Afshar, K. N. Plataniotis, and A. Mohammadi, "Capsule Networks for Brain Tumor Classification Based on MRI Images and Coarse Tumor Boundaries," *ICASSP, IEEE Int. Conf. Acoust. Speech Signal Process. - Proc.*, 2018, doi: 10.1109/ICASSP.2019.8683759.